Journal of Food Technology Research
2025 Vol. 12, No. 2, pp. 84-101
ISSN(e): 2312-3796
ISSN(p): 2312-6426
DOI: 10.18488/jftr.v12i2.4208

Mathematical modeling and experimental study of heat and mass transfer in cupcake baking using an air fryer

Boussaha Soumia[1,2+]
Haddad Djamel[3]
Djaraoui Afaf[4]
Baississe Salima[1]

[1]*Food Science Laboratory, Food Engineering Department. Institute of Agriculture and Veterinary Sciences, University Hadj Lakhdar. Batna1. Biskra Avenue, Batna, 05000, Algeria.*
[2]*Laboratory of Biological Engineering, Valorization, and Innovation of Food Products, ISTA-Ain M'lila Institute, Larbi Ben M'hidi University, Oum El-Bouaghi, Oum El-Bouaghi 04000, Algeria.*
[1,2]*Email: soumia.boussaha@univ-oeb.dz*
[1]*Email: salima.baississe@univ-batna.dz*
[3]*Health and Safety department, Faculty of Engineering Sciences, University Batna2, Batna, Algeria.*
[3]*Email: d.haddad@univ-batna2.dz*
[4]*Basic Education in SM Department, Faculty of Sciences, University Batna1, Batna, Algeria.*
[4]*Email: afaf.djaraoui@univ-batna.dz*

(+ Corresponding author)

Article History
Received: 28 March 2025
Revised: 21 April 2025
Accepted: 30 April 2025
Published: 13 May 2025

Keywords
Air fryer
Baking
Experimental validation
Heat and mass transfer
Mathematical modeling
Phase transition
Volume expansion.

ABSTRACT

Baking involves simultaneous heat and mass transfer, alongside physical and chemical transformations that determine product quality. While conventional baking has been extensively modeled, air fryer baking remains underexplored, despite its growing popularity as a healthier alternative. This study aims to develop and experimentally validate a mathematical model describing heat and mass transfer during cupcake baking in an air fryer. The model incorporates forced convection, conduction, thermal radiation, gas release, and porosity evolution. It also integrates the simulation of the cooking value (CV), a parameter analogous to the sterilization value, to standardize heat treatment assessment. To validate the model, experimental baking trials were conducted, with color changes used as a key quality indicator. The results showed strong agreement between simulated and experimental data, confirming the model's reliability in predicting temperature profiles, porosity, moisture loss, gas generation, and browning kinetics. Color measurements further validated the model, achieving a high coefficient of determination (R^2=0.996). These findings demonstrate the air fryer's efficiency in reducing baking time while ensuring optimal quality. The model provides a valuable framework for optimizing heat and mass transfer in modern baking and can be extended to other processes involving phase transitions and volume changes, such as drying and extrusion cooking.

Contribution/Originality: This study is the first to develop a numerical model for heat and mass transfer during baking in an air fryer, which has not been explored before. It also represents the first attempt to model the cooking value (CV), a parameter that has not been modeled in baking processes previously.

1. INTRODUCTION

Baking is a key step in food preparation. It is a complex process involving heat and mass transfer along with various physical, chemical, and biological transformations. These changes include water evaporation, volume expansion, porosity structure development, starch gelatinization, protein denaturation, crust formation, and the

Maillard reaction (Sakin-Yilmazer, Kaymak-Ertekin, & Ilicali, 2012). An enhanced understanding of these mechanisms is essential for optimizing baking conditions and ensuring high product quality (Mosalam, 2021).

Cupcakes, widely popular bakery products, undergo significant heat and mass transfer during baking (Seranthian & Datta, 2023). Studying these mechanisms is crucial to controlling the final shape, size, texture, and color of the cake (Cevoli, Panarese, Catalogne, & Fabbri, 2020; El Helou, Le Bideau, Fuentes, & Glouannec, 2024). A better understanding of these processes leads to advancements in baking techniques and optimization strategies based on logical foundations (El Helou, Bideau, Fuentes, & Glouannec, 2024).

Mathematical modeling serves as an efficient and practical approach for pre-design, optimization, and process control in baking, reducing the reliance on lengthy trial-and-error experiments to achieve superior quality outcomes (Sakin, Kaymak-Ertekin, & Ilicali, 2007). Baking process models typically incorporate heat and mass transfer equations, including convective and radiative heat transfer at the surface, internal heat conduction, moisture diffusion in liquid and vapor phases, internal and surface evaporation, and convective moisture removal (Cevoli et al., 2020).

Research on modeling and simulation of cake baking continues to attract interest due to the complexities associated with describing the coupled heat and mass transport phenomena (El Helou et al., 2024; Mosalam, 2021). While several studies have explored mathematical models for cake baking, the majority have focused on conventional baking methods such as griddle, pan, and oven (Khatir et al., 2012; Li, Liu, Xie, & He, 2015; Yang et al., 2025), leaving a gap in understanding baking dynamics in alternative technologies such as air fryers.

The air fryer has gained popularity as a new way of preparing healthy food, eliminating the need for added oil (Lee & Lee, 2024). This equipment uses both natural and forced convection, where circulating heated air facilitates cooking food at high temperatures; hot air helps to maintain a homogeneous temperature (Murzaini, Taip, Ab Aziz, & Abd Rahman, 2020). Additionally, thermal radiation from the air fryer's heating elements enhances heat exchange, making it suitable for baking different products, including cakes. Furthermore, some studies suggest that baking with an air fryer with fast airflow can lead to moist, high-quality cakes while allowing for lower baking temperatures and shorter baking times compared to traditional ovens (Mior Zakuan Azmi, Taip, Mustapa Kamal, & Chin, 2019).

This study aims to contribute to overcoming the existing research gap by investigating a mathematical model for cupcake baking in an air fryer. The insights gained from this study will help optimize baking parameters to enhance product quality. The air fryer, with its efficient heat circulation and fast frying capabilities, is crucial for ensuring consistent baking. Moreover, color change is a significant quality indicator that provides information about the heat and mass transfer dynamics during the baking process. Experiments were carried out under a variety of baking conditions to determine this parameter. The results were used to validate our model, demonstrating the effectiveness of simulations in predicting the color changes during baking. The findings of this study will help optimize baking parameters to improve product quality and efficiency.

2. MATHEMATICAL MODEL

2.1. Problem Description and Assumptions

Heat and mass transfer in an air fryer differ significantly from a conventional oven due to the continuous circulation of hot air at high speeds (Azmi, Ahmedov, & Taip, 2020). While many existing studies focus on natural convection (El Helou et al., 2024; Li et al., 2015; Seranthian & Datta, 2023), they often overlook the impact of forced convection and thermal radiation, which play a key role in an air fryer. To enhance accuracy, our model explicitly includes forced convection in both heat and mass transport, while also accounting for thermal radiation from the air fryer's walls, which contributes to the total heat exchange. This approach results in a more accurate simulation of the baking process.

To better understand the air frying process, Figure 1 presents a simplified description of the air fryer and how it functions. Within the device, a heating element and a fan work together to generate and circulate hot air. The cupcake, assumed to be spherical, is placed on a perforated plate that allows air to flow from all sides, ensuring even cooking.

During baking, heat transfer, moisture loss, and gas release cause the batter to expand and progressively change its texture.

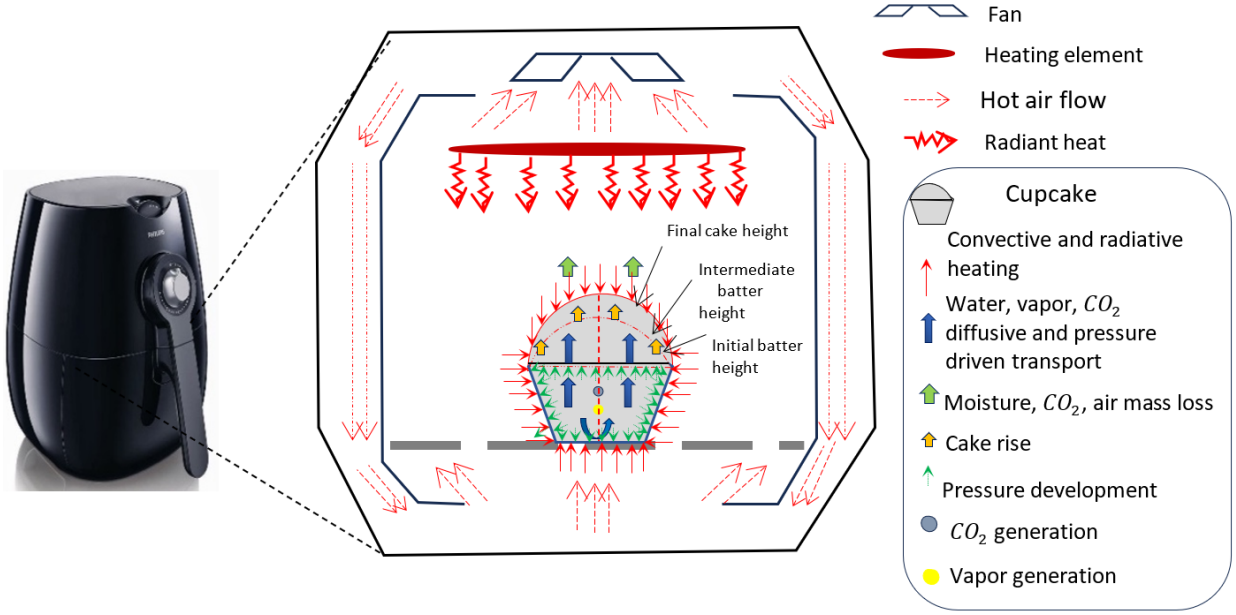

Figure 1. Thermal and mass transfer mechanisms in cupcake baking using an air fryer.

Baking cupcakes in an air fryer occurs under convection, conduction, and radiation. The fan circulates hot air to cook the cupcake uniformly, allowing heat to penetrate the layers and bake the center. At the same time, radiation helps to brown the surface and accelerate moisture evaporation. The model assumes that steam and liquid water diffuse separately. As heat enters the batter, moisture evaporates and causes the batter to expand. Chemical reactions such as the Maillard reaction and caramelization enhance flavor and color. Thus, the combination of heat, moisture movement, and chemical reactions results in a perfectly baked cupcake.

2.2. Governing Equations

During cupcake baking, the heat transfer inside the batter is treated as a transient heat transfer problem that includes conduction, convection, and radiation, along with phase change due to water evaporation. Table 3 provides the nomenclature of all symbols and parameters used in the mathematical model.

2.2.1. Heat Transfer

The heat transfer problem with phase change in muffin batter, based on the principle of energy conservation, is given by.

$$\rho_p c_{p,p} \frac{\partial T}{\partial t} = \nabla(k_p \nabla T) - \rho_s R_{evp} H_{evp} \quad (1)$$

Where T is temperature (K), t is time (s), k_p is thermal conductivity of the product $(W/m.K)$, $c_{p,p}$ is specific heat capacity of the product (J/kg), and ρ_p and ρ_s are the densities of the product and the dry solid (kg/m^3), respectively, H_{evp} is the latent evaporation heat (J/kg) and R_{evp} is the evaporation rate (kg Water/ (kg solids)). The second term on the right side of Equation 1 accounts for local water evaporation and represents the heat loss associated with this phase change.

2.2.2. Mass Transfer

The mass transfer equation governing the transport of both liquid water (C_l) and water vapor (C_v) in the batter, considering evaporation effects, can be expressed as.

$$\frac{\partial C_l}{\partial t} = \nabla(D_l \nabla C_l) - R_{evp} \quad (2)$$

$$\frac{\partial C_v}{\partial t} = \nabla(D_v \nabla C_v) + R_{evp} \quad (3)$$

Where C_l and C_v are the liquid water and vapor content on a dry basis (kg water/kg solid), respectively, D_l and D_v are the liquid and vapor diffusion coefficients (m^2/s), respectively. The sign of R_{evp} in Equation 2 and 3 indicates the phase change dynamics: a negative value represents a decrease in the liquid, while a positive value corresponds to an increase in the vapor.

The evaporation rate (R_{evp}) is modeled as a heterogeneous reaction following first-order kinetics (Feyissa, Gernaey, Ashokkumar, & Adler-Nissen, 2011) where liquid water transforms into water vapor. This rate is governed by the Arrhenius equation, accounting for temperature dependency and variations in water content. Since evaporation primarily occurs near the evaporation temperature (T_{evp}), the evaporation rate is strongly influenced by temperature variations and mass transfer resistance. A modified velocity equation is used to better represent rapid phase changes and specific evaporation effects that are not always well captured by the standard Arrhenius equation (Feyissa, Gernaey, & Adler-Nissen, 2012). The modified velocity equation for the evaporation rate near the evaporation temperature, is given by.

$$R_{evp} = k'_{evp} C_1 \quad (4)$$

With

$$k'_{evp} = k_{evp}\, exp\left(-\frac{E_a}{R}\left(\frac{1}{T} - \frac{1}{T_{evp}}\right)\right) \quad (5)$$

Where E_a is the activation energy (J/mol), R is the gas constant $(J/K.mol)$, k_{evp} is the evaporation constant at the evaporation temperature $(1/s)$.

Cupcake baking produces volume expansion due to gas generation, vapor water formation, and structural transformations. In order to simplify the problem, we suppose that the cupcake maintains a spherical shape from the initial batter stage to the final baked product. Initially, the batter has a volume V_0.

$$V_0 = \frac{4}{3}\pi r^3 \quad (6)$$

Where r represents the initial radius of the cupcake.

Several models have been proposed in the literature to describe the expansion of baked products during baking. Zhang, Datta, and Mukherjee (2005) constructed a polynomial equation (Equation 8) to fit the experimental data presented by Nicolas et al. (2010). Equation 7 gives the radius augmentation.

$$dR = \sqrt{\frac{V_0.\alpha}{\pi}} \quad (7)$$

α is the volume fraction, defining by.

$$\alpha(t) = \begin{cases} \begin{bmatrix} -2.10^{-4}.t^5 + 5.10^{-3}.t^4 - 4{,}49.10^{-4}.t^3 \\ +0{,}1517.t^2 + 4{,}810^{-3}.t + 0{,}9968 \end{bmatrix} & \text{if } t \le 6\,min \\ \alpha = 1{,}7132 & \text{if } t > 6min \end{cases} \quad (8)$$

Leading to a new volume.

$$V = \frac{4}{3}.\pi.(r + dR)^3 \quad (9)$$

The Porosity ε is a crucial parameter that must be analyzed during the cupcake baking process due to its significant impact on texture and structure, defining as.

$$\varepsilon = \frac{V - V_0}{V} \quad (10)$$

Changes in food quality during baking depend on both time and temperature. By analogy with the sterilization value, these effects are described by the cooking value (CV), which quantifies the overall thermal impact of a process. This value is defined with a reference temperature of 100°C and an average z-factor of 30°C, allowing different cooking methods to be compared using a common standard (Bazinet & Castaigne, 2019). It is expressed as.

$$CV = \int 10^{\frac{T(t) - T_{ref}}{z}} . dt \quad (11)$$

Where $T(t)$ represents temperature variation over time intervals dt.

2.2.3. Thermo-Physical Properties

Due to the high heterogeneity of food systems, it is impossible, or at least very difficult, to determine the exact material properties of a specific sample. For instance, two different cupcakes may have different formulations due to variations in ingredients. For this reason, many modeling and simulation studies rely on adjusted material properties that are adapted for the specific case under study.

The present work considers the use of well-known empirical correlations to calculate effective properties for cupcakes, such as density and heat capacity, as functions of local temperature. These parameters are both essential in mass and energy balance equations. The total mass of each component is determined by integrating mass concentration over the entire volume domain, while the mixture density is computed using a weighted parallel model based on mass fractions. Similarly, the heat capacity is determined using the same weighted approach, confirming an accurate representation of the thermal properties of the system. They are presented in Table 1 (Appendix).

This approach is particularly advantageous when considering reacting mixtures, which is the main reason for its selection: One of the objectives of this study is to provide a model that can be readily applied to cases where chemical reactions cause significant regional variations, such as browning and CO_2 formation.

The solid phase of the system is characterized by its macrocomponents, such as proteins, carbohydrates, ash, fibers, and fats. However, this approach can be extended to more specific components, depending on the needs of future applications.

2.3. Boundary Conditions for Heat and Mass Transfer

During baking, the movement speed of the fluid gradually decreases in the direction towards the surface due to viscous forces. As baking progresses, heat is transferred by convection, as the surrounding hot air circulates, and by radiation, as the surface absorbs thermal energy. Therefore, the heat transfer at the surface is governed by the following equation.

$$n.(-k.\nabla T) = -h_t(T - T_b) + \sigma.\varepsilon_r.(T^4 - {T_b}^4) \quad (12)$$

Where

σ is the Stefan-Boltzmann constant (W/m^2K^4),

ε_r is the emissivity,

h_t (W/m^2K) represents the heat transfer coefficient, it was determined by the correlation considering the process parameters using the following equations.

$$h_t = \frac{Nu.k}{L} \quad (13)$$

For natural and forced convection, the heat transfer is governed by the dimensionless numbers thermal Grashof (Gr_t) , Prandlt (Pr), and Rayleigh (Ra).

$$Gr_t = \frac{g.\beta_t.L^3.{\rho_a}^2.(Ts - T_b)}{\mu_a} \quad (14)$$

$$Pr = \frac{cp_a.\mu_a}{k} \quad (15)$$

$$Ra = Gr_t.Pr \quad (16)$$

The Nusselt number (Nu) differs based on the dominant convection mode. For natural convection, Nu is expressed as given in Equation 17, while for forced convection, it corresponds to Equation 18.

$$Nu_{natural} = 0.54Ra^{0.25} \quad (17)$$

$$Nu_{forced} = 0.023.Re^{0.8}.\ Pr^{0.3} \quad (18)$$

Inside the cupcake, there is no heat transfer between the muffin's center and the surrounding fluid. In this case, only conduction exists following the equation.

$$n.(-k.\nabla T) = 0 \quad (19)$$

Concerning mass transfer, at the upper surface, the boundary conditions for liquid water and liquid steam are given by.

$$n.(-D.\nabla C) = -h_m(C - C_f) \quad (20)$$

Where C_f is the hot air fraction, C represents liquid water C_l and water vapor C_v fractions.

The mass transfer coefficient $h_m\ (m/s)$ was determined using the established Chilton-Colburn analogy, which correlates the Nusselt number with the Sherwood number (sh) as.

$$h_m = \frac{Sh.D_a}{L} \quad (21)$$

The dimensionless numbers used for natural convection regime are.

$$Sh_{natural} = 0.54(Ra_m)^{1/4} \quad (22)$$

With $Ra_m = Gr_m.Sc$

$$Sc = \frac{\mu_a}{\rho_a.D_a} \quad (23)$$

$$Gr_m = \frac{g.L^3.{\rho_a}^2.(C - C_\infty)}{\mu_a} \quad (24)$$

And for forced convection regime.

$$Sh_{forced} = 0.023\,Re^{0.8}.Sc^{0.3} \quad (25)$$

$$Re = \frac{\rho_a.u.L}{\mu_a} \quad (26)$$

Where Gr_m and Re are mass Grashof and Reynolds numbers, respectively, u is the fan velocity in the air fryer.

3. NUMERICAL METHOD

The governing equations and boundary conditions described in the previous section were implemented in a transient 1D axisymmetric model to simulate heat and mass transfer during baking. The model assumes that temperature $T(t,x)$ and concentration $C(t,x)$ fields are uniform along the spatial coordinate x. To simplify the problem, the equations were integrated over the domain [0, L], effectively eliminating the spatial dependency and applying an averaging technique over the studied region.

$$\frac{\partial T}{dt} = \frac{1}{\rho c_p L}\left[-h_t(T - T_b) + \sigma.\varepsilon_r.(T^4 - {T_b}^4) + \rho_s H_{evp}.L.R_{evp}\right] \quad (27)$$

$$\frac{\partial C_l}{dt} = -\frac{h_m}{L}(C_l - C_{l,air}) - R_{evp} \quad (28)$$

$$\frac{\partial C_v}{dt} = -\frac{h_m}{L}(C_v - C_{v,air}) + R_{evp} \quad (29)$$

The numerical resolution was performed using the Euler method transient approach. MATLAB was used to implement the computational model and solve the governing equations. The numerical scheme ensures stability and convergence while accurately capturing the key transport phenomena occurring during the baking process.

To discretize the governing equations, the time-discretized form at time step *t(k)* is given by.

$$T_{(k+1)} = T_{(k)} + \frac{\Delta t}{\rho c_p L}.\left[-h_t(T_{(k)} - T_b) + \sigma.\varepsilon_r.(T_{(k)}^4 - T_b{}^4) + \rho_s H_{evp}.L.R_{evp}\right] \quad (30)$$

$$C_{l_{(k+1)}} = C_{l_{(k)}} + \Delta t.\left(-\frac{h_m}{L}(C_{l_{(k)}} - C_{l,air}) - R_{evp}\right) \quad (31)$$

$$C_{v_{(k+1)}} = C_{v_{(k)}} + \Delta t.\left(-\frac{h_m}{L}(C_{v_{(k)}} - C_{v,air}) + R_{evp}\right) \quad (32)$$

4. RESULTS AND DISCUSSION

4.1. Dynamics of Heat Transfer During Baking

4.1.1. Temperature Profiles

Baking in air fryers, like all baking methods, begins by heating the liquid dough until it forms a stable foam. Through the process, the batter undergoes several successive phases that influence the final texture and color of the product. Understanding the temperature profiles during cupcake baking is essential for controlling these transformations and optimizing the final quality. Figure 2 represents the temperature evolution during baking. We notice that each profile can be divided into three distinct phases. The first is the initial phase, where the temperature gradually increases. This faster rise occurs more rapidly at higher baking temperatures due to the significant temperature gradient between the batter and the hot air in the baking chamber. The second is the rapid heating phase, during which heat transfer accelerates, resulting in a rapid increase in temperatures. Finally, the plateau phase is reached, where the temperature rises very slightly, indicating a near steady-state condition. This behavior can be explained by the fact that evaporation intensifies as the temperature approaches 100°C. The rate of temperature increase slows down as more energy is used for evaporation at the cupcake's surface. When water content becomes low, and since starch retains moisture, evaporation diminishes, allowing the temperature in dry regions to exceed 100°C. When the baking temperature is set to 160°C, the internal temperature gradually reaches about 150°C after 20 minutes. However, this increase is slower compared to baking at higher temperatures: At 180°C and 200°C, the internal temperature of 150°C is reached in just 8 and 3 minutes, respectively. The effect of forced convection becomes more noticeable at these higher temperatures, significantly reducing the time needed to reach a similar internal temperature.

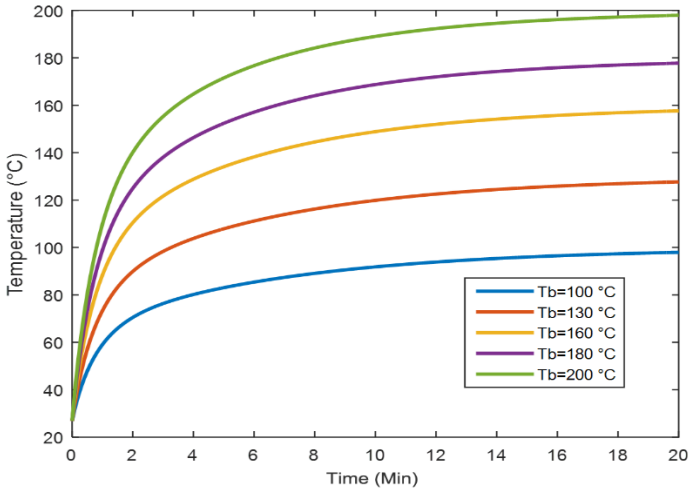

Figure 2. Temperature evolution during baking for different baking temperatures (Tb).

4.2. Comparative Analysis of Heat Transfer Mechanisms

Figure 3 shows the temperature evolution over time under different heat transfer modes: forced convection with and without radiation, as well as natural convection with and without radiation. It can be observed that forced convection combined with radiation results in the fastest temperature rise. This acceleration is due to two key factors: first, forced convection improves heat transfer by rapidly renewing the hot air layer surrounding the product; second, radiation directly heats the food's surface, further intensifying the heating process.

In an air fryer, these two mechanisms are predominant, which explains why food cooks faster compared to other conventional cooking methods. Indeed, an air fryer maximizes forced convection by maintaining a high-speed hot air flow, promoting efficient and uniform heat transfer. As a result, temperature curves for forced convection show a rapid rise, while those for natural convection indicate a slower, more gradual warming.

The effect of radiation is also visible: when radiation is taken into account, the temperature rises even more rapidly, especially in forced convection, where it amplifies the heat transfer efficiency. This synergy between convection and radiation is a defining feature of air fryers, making them significantly more effective than traditional ovens in terms of reducing baking time.

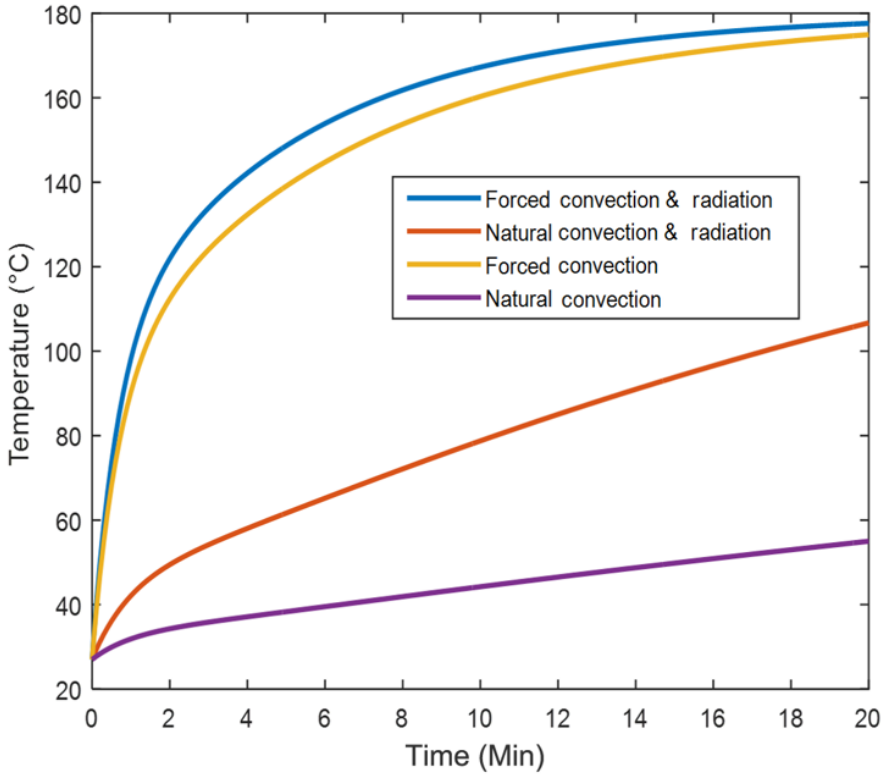

Figure 3. Influence of convection and radiation on temperature rise during baking, Tb=180°C.

5. PHASE TRANSITIONS AND GAS EMISSION

5.1. Effect of K_{evp} on the Vapor and Liquid Fractions during Baking

The rate of water evaporation from the dough is described by the evaporation constant, k_{evp}. This constant is influenced by several factors, such as baking temperature, dough composition, and evaporation surface. To highlight its role in baking, multiple simulations were conducted to analyze the kinetic behavior of water, tracking both liquid and vapor fractions over time for different k_{evp} value. Figure 4, illustrates these variations, showing (a) the vapor fraction and (b) the liquid fraction during baking. The results display that an increase in k_{evp} accelerates water evaporation, in consequence, a rapid phase transition from liquid to vapor occurs as thermal energy converts liquid water to steam.

In Figure 4b, the liquid fraction decreases more rapidly at higher k_{evp} values, indicating a faster depletion of water in the dough. This behavior can be attributed to the fact that at higher baking temperatures or with an increased evaporation surface, the energy supplied to the system enhances the kinetic energy of water molecules, promoting their escape from the liquid- phase into the gas phase. Additionally, capillarity forces within the dough matrix become weaker as the water content decreases, further accelerating evaporation.

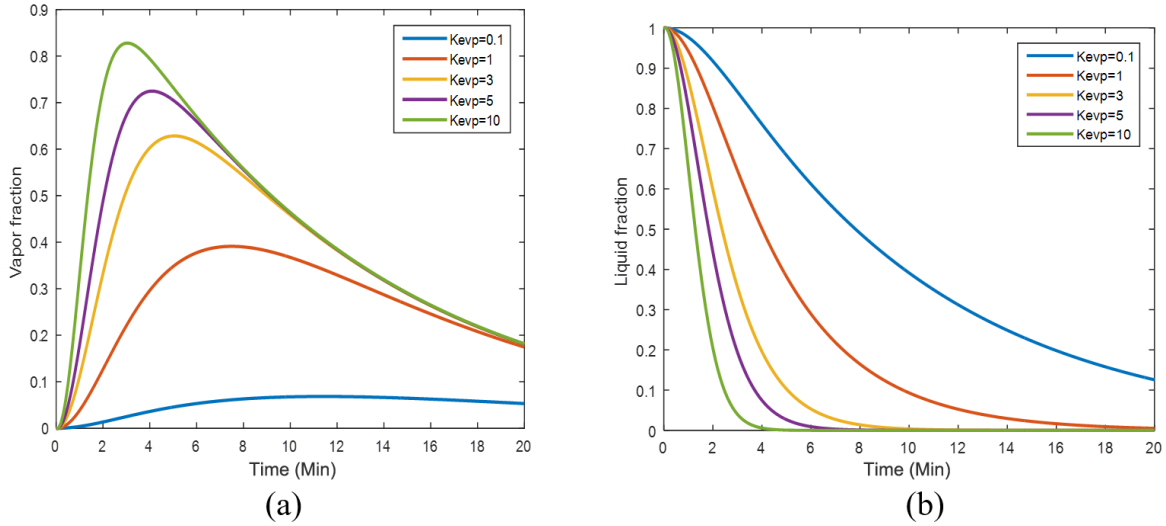

Figure 4. Evolution of vapor and liquid fractions over time as a function of the evaporation coefficient, $(k_{evp} \times 10^{-5} s^{-1})$.

Simultaneously, Figure 4a shows a significant rise in the vapor fraction, which aligns with the increase in the evaporating water fraction. Interestingly, even when most of the liquid water has evaporated (with the liquid fraction approaching zero), the vapor fraction does not reach 1. This suggests that gas production, especially carbon dioxide (CO_2), has not yet reached its maximum level. This is a result of ongoing reactions in the dough during baking, such as fermentation or thermal degradation.

5.2. Evolution of Phase Transitions and (CO_2) Emission Over Time

During baking, chemical reactions such as fermentation and thermal decomposition contribute to carbon dioxide (CO_2) production. A comparison of the liquid, vapor, and CO_2 fractions Figure 5 shows that the water evaporation and vapor formation do not directly complement each other. Instead, as liquid water diminishes, CO_2 progressively replaces it, following the principal of mass conservation $(1 - C_l - C_v)$. This ensures that the total sum of the three fractions remains constant throughout the process.

The fact that the vapor fraction never reaches 100%, even after all liquid water has evaporated, suggests that gas distribution within the dough remains heterogeneous. Unlike water, which evaporates quickly, CO_2 diffuses at a slower rate due to the porosity and structural complexity of the dough matrix. This difference in diffusion rates highlights the role of the dough's physical properties influence gas retention and release during baking.

The curves show that at the first stage of baking, the liquid fraction declines sharply, reaching nearly zero within 7-8 minutes, reflecting rapid moisture loss. Simultaneously, the vapor fraction rises and peaks around 5-6 minutes, then steadily decreases as CO_2 production grows. Also, the CO_2 fraction gradually increases and eventually exceeds the vapor fraction. This delayed rise in CO_2 illustrates that gas retention plays a vital role in determining the final texture and volume of the baked product.

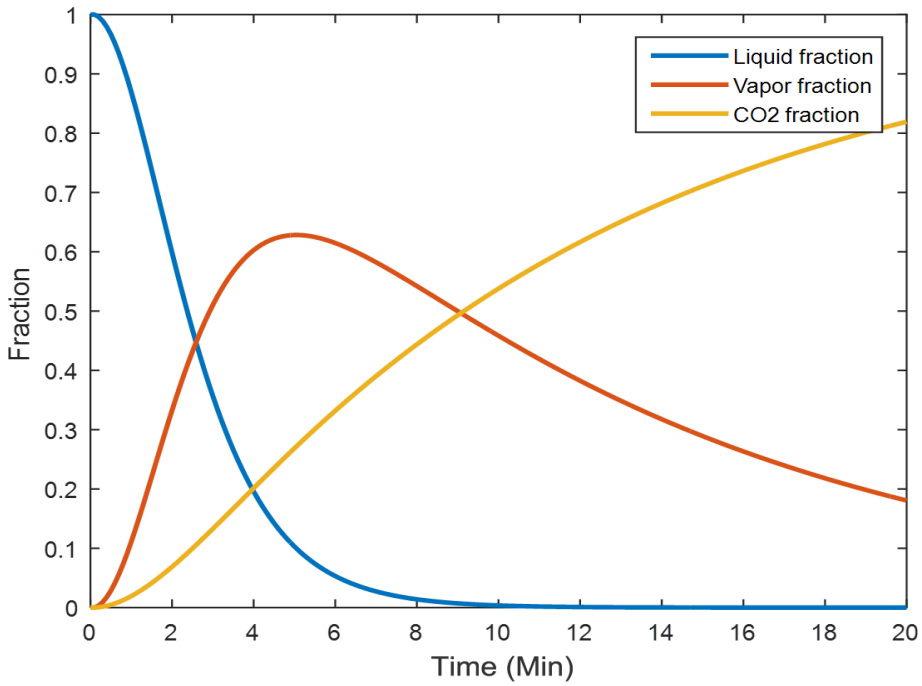

Figure 5. Evolution of liquid, vapor, and CO_2,fractions during baking, Tb=180°C.

6. IMPACT OF POROSITY CHANGES ON HEAT TRANSFER

The porosity of cupcakes is a crucial parameter as it provides insight into the quality of the product. The variation in porosity during baking is plotted in Figure 6. The results show that porosity increases rapidly during the first few minutes of baking, then evolves and stabilizes at an asymptotic value of 0.35 (meaning air occupies 35% of the total volume), the final volume expansion occurs within 6 minutes. This phenomenon is explained by the reaction between heat, moisture and the chemical leaving agent, which produces carbon dioxide CO_2, causing pores formation in the batter and inducing its expansion.

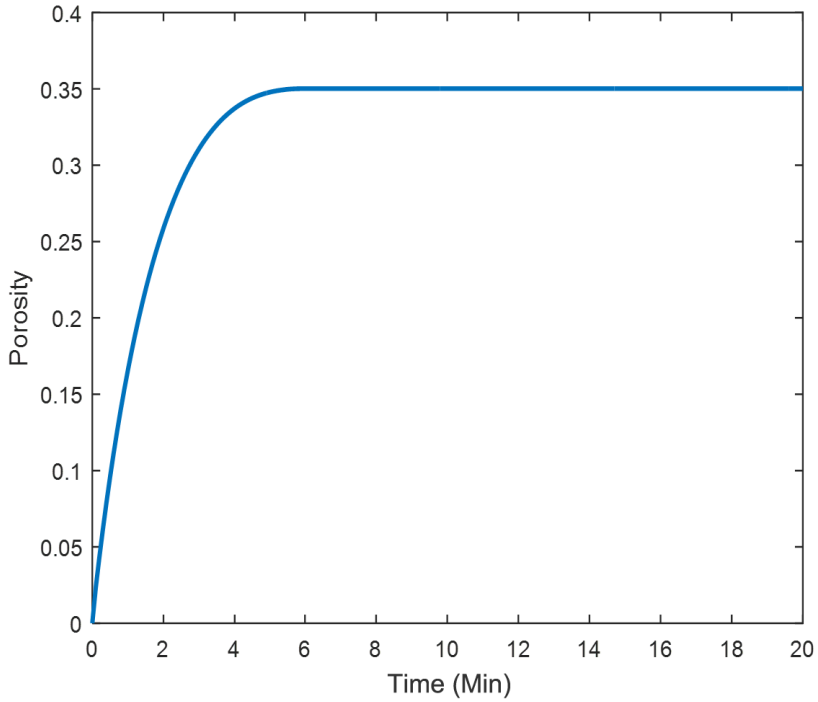

Figure 6. Evolution of porosity during baking.

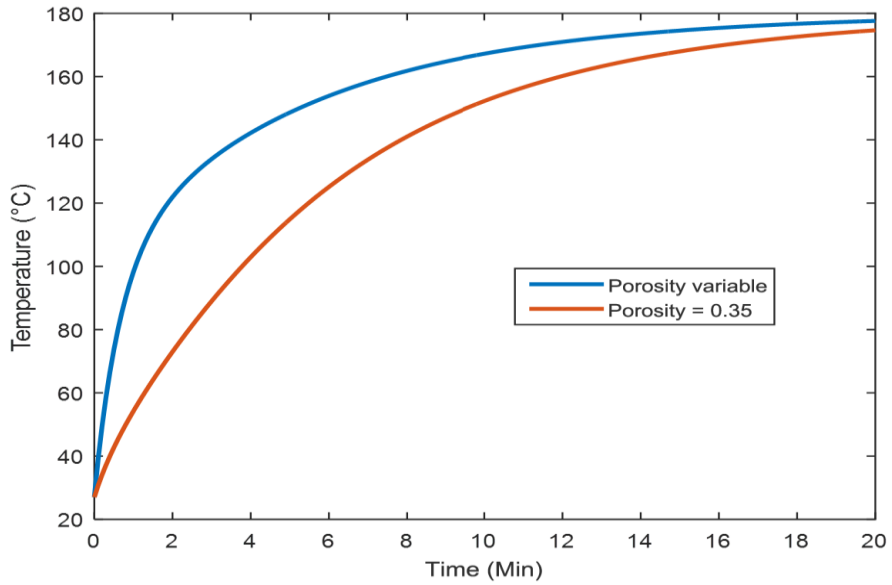

Figure 7. Evolution of temperature during baking for variable and constant porosity, Tb=180°C.

To analyze the effect of porosity on heat and mass transfer, the temperature evolution over time was plotted based on simulations for both variable porosity (calculated in the model) and assumed constant porosity (i.e., neglecting volume change). The results are presented in Figure 7. We observe that temperature increases more rapidly when porosity is variable, highlighting the importance of porosity modeling in predicting heat transfer.

Since porosity is initially low, the solid thermophysical properties are dominant, leading to a rapid temperature increase. However, once the porosity stabilizes, heat transfer becomes less effective, as the trapped air in the pores acts as an insulator.

7. IMPACT OF THE EVAPORATION RATE ON THE COOKING VALUE

As discussed previously, cupcakes do not immediately reach the target temperature. Initially, they gradually warm up from ambient to baking environment temperature. Then, heat is transferred by conduction from the surface to the core of the product. To take into account these thermal accumulation effects, the cooking value expresses the equivalent time that the food would have passed at 100°C, standardizing the evolution of heat treatments, even when cooking profiles differ.

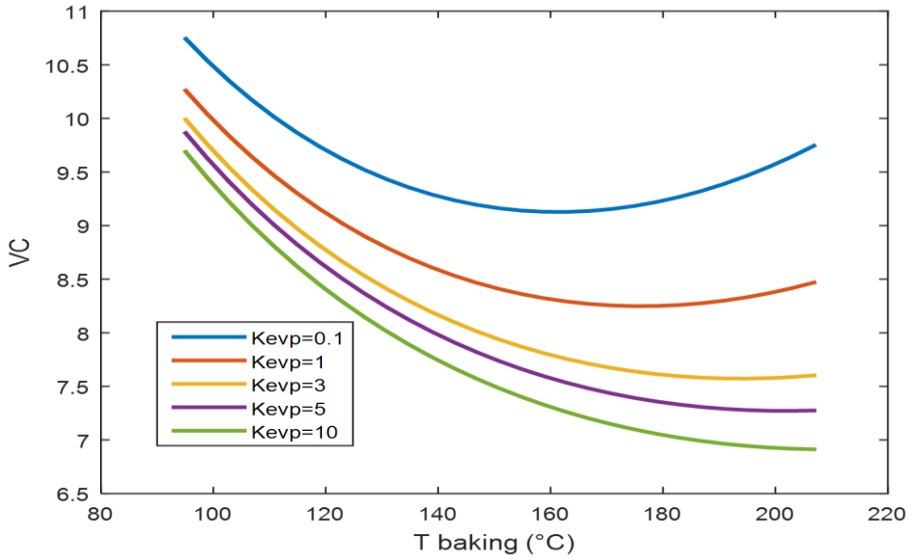

Figure 8. Variations for CVas a function of baking temperature for different (k_{evp}) values, $(k_{evp} \times 10^{-5} s^{-1})$.

Figure 8 presents the simulations of CV profiles for different values of k_{evp}. For low values of k_{evp} $(0.1 \times 10^{-5}/\text{s})$ to $(3 \times 10^{-5}/\text{s})$, CV remains high even elevated temperatures. In contrast, for higher values of k_{evp} $(3 \times 10^{-5}/s)$ to $(5 \times 10^{-5}/s)$, CV decreases more significantly. This can be attributed to the fact that rate determines how quickly a substance transition into vapor at a given temperature.

The evaporation rate is a measure of how quickly a substance can change into vapor at a given temperature and pressure (Mołczan & Cyklis, 2023). k_{evp} value indicates faster evaporation and heat transfer, due to forced convection effect, which enhances heat transfer efficiency, and accelerates phase change. A higher k_{evp} facilitates better heat transmission to the product and ultimately reduces the cooking time.

8. EXPERIMENTAL MEASUREMENT OF COLOR CHANGE FOR MODEL VALIDATION

The variation in color (ΔE) is a crucial aspect of a cupcake's appearance, serving as a physical indicator of how different baking methods influence the baking process.

To verify the accuracy of the numerical model, baking experiments were conducted using a commercial air fryer (Tefal XXL). Throughout the baking process, color variation (ΔE) measurements were realized with a Chroma Meter CR-5 (Laboratory of Analysis, Valorization, and Food Safety, University of Sfax, ENIS, Tunisia). The Chroma Meter provided the L (lightness), a (redness), b (yellowness) color parameters. The Baking duration was set to 15 minutes, based on preliminary tests that identified the most suitable baking conditions. The experiments were carried out at 160°C and 180°C, with color measurements taken every three minutes. To ensure reliable results, each measurement was repeated three times, and the average value was used to minimize experimental errors.

The total color difference ΔE was then determined using the following equation.

$$\Delta E = \sqrt{(L^* - L_0)^2 + (a^* - a_0)^2 + (b^* - b_0)^2} \quad (33)$$

Where L_0, a_0, and b_0 represent the initial color values, while L^*, a^*, and b^* correspond to the color values of the cupcake's crust after baking.

The collected data, using Equation 33, was interpolated to obtain ΔE values at any time beyond the discrete experimental points. The computed values were then compared with the experimental data to assess their reliability. Table 1 provides an overview of the experimentally recorded ΔE values at different baking times for both baking temperatures.

Table 1. Experimental data for color variation (ΔE) during baking.

Time (Min)	ΔE	
	160°C	180°C
3	4.47	5.48
6	5.1	6.78
9	5.39	6.9
12	5.57	7.28
15	5.74	7.45

To refine this analysis, a mathematical expression was derived to more accurately represent the experimental measurements, yielding in the following expression.

$$\Delta E = (a + b.T).(1 - e^{-k.t}) \quad (34)$$

Where a and b are coefficients related to the system's properties, t represents time, and k is a kinetic coefficient determined using Arrhenius expression (Zanoni, Peri, & Bruno, 1995).

$$k = k_0.\exp(-Ea_{color}/R.T) \quad (35)$$

Here k_0 and Ea_{color} are constants defining the browning process, R is the universal gas constant, and T is the absolute temperature in kelvin. Since direct surface temperature measurement of the cupcakes was challenging, T was assumed to be the baking temperature.

The coefficient of determination (R^2) was calculated to evaluate the interpolation model's accuracy. A model with an R^2 value of 0.80 is considered well-fitted. Table 2 displays the fitted equation parameters obtained for each baking temperature. The high R^2 values (> 0.99) imply that it accurately predicts color changes during baking.

Table 2. Interpolation model parameters and fit accuracy.

a	b	k_0	Ea_{color}	R^2
-31.6636	0.0859	0.0031	$3.369.10^3$	0.996

Figure 9 illustrates the evolution of ΔE over time at two baking temperatures, (160°C and 180°C), comparing the experimental values with those predicted by the mathematical model. A strong correlation is observed between both datasets, with a coefficient of determination $R^2 = 0.996$ confirming the reliability of the proposed model.

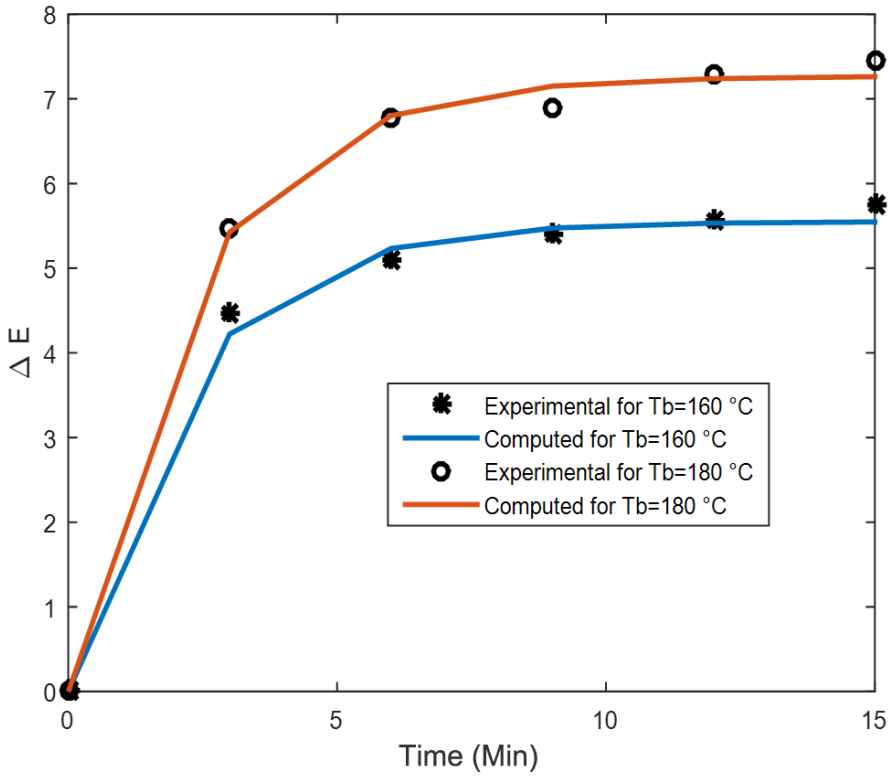

Figure 9. Comparison of experimental and computed ΔE values at 160°C and 180°C during baking.

However, while this approach provided a good fit to the experimental data, one notable observation emerges in the early stages of baking. The simulation predicts an immediate change in ΔE, whereas, in reality, browning does not start promptly. This difference arises because the baking temperature was directly assigned as the initial temperature of the product, instead of accounting for its gradual increase over time.

This highlights the significance of heat transfer modelling, where all modes of transfer (conduction, convection, radiation) and phase change must be integrated to accurately determine the product's temperature evolution.

To incorporate this thermal dependency, we integrated the interpolated ΔE equation with the developed model, where the temperature changes over time. Figure 10 presents the simulations of ΔE over time for different temperature baking

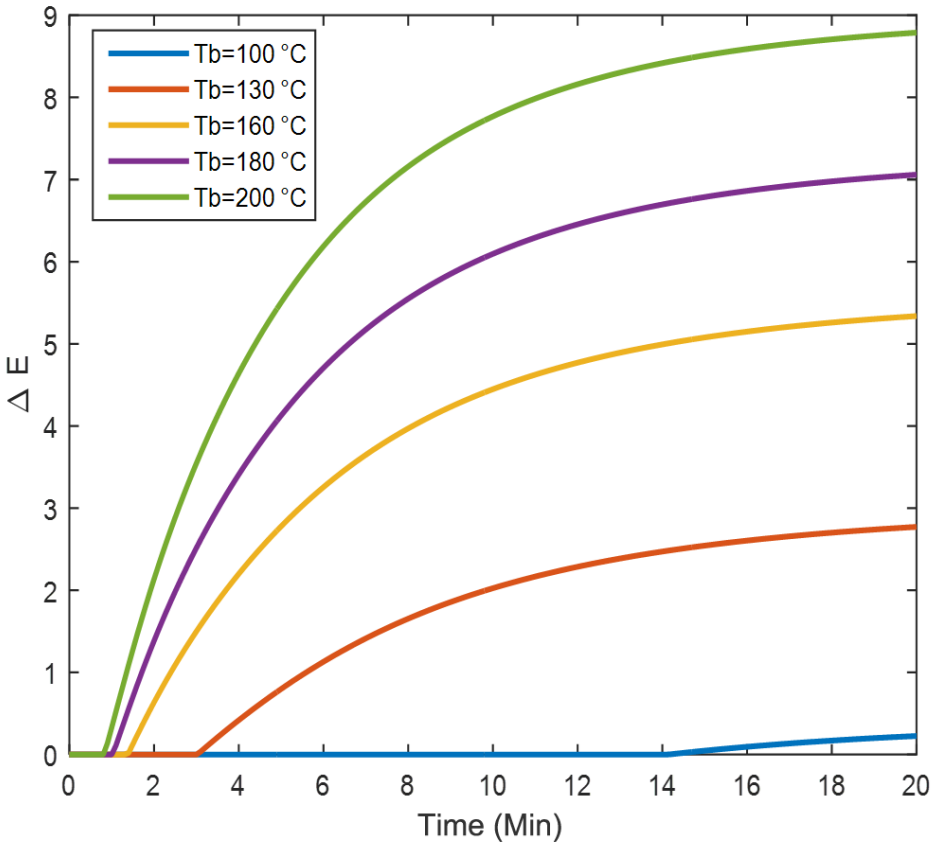

Figure 10. Effect of baking temperature on cupcake color variation.

The analysis of the cupcake color evolution (ΔE) as a function of time and baking temperature Figure 10 highlights the role of heat and mass transfer in the browning process. The results indicate that baking temperature significantly influences the rate and intensity of color change.

Higher temperatures accelerate the browning reactions, leading to more pronounced color development. At 200°C, ΔE increases sharply, reaching a plateau after 15 to 20 minutes, indicating that the browning reactions have fully developed. At 180°C, the trend is similar but slightly less intense, indicating a slower yet effective browning process. At 160°C, ΔE rises more gradually, with a lower maximum value, reflecting a reduced reaction rate due to limited thermal energy. However, at 130°C and below, ΔE remains minimal, suggesting that the temperature is insufficient to initiate significant browning reactions. Browning does not start immediately after exposure to the heat, rather, it begins after a certain period. To further investigate this relationship, we compared the browning latency period (before ΔE starts increasing) with the temperature kinetics curve (Figure 2). The analysis revealed that for each baking temperature, the latency period corresponds to the time required for the product's internal temperature to reach 90°C. This temperature is particularly significant as it coincides with the gelatinization of starch, a key transformation that influence the texture and moisture distribution within the product. Higher baking temperatures accelerate Maillard reactions and caramelization, leading to a faster and more intense browning. However, browning only begins once the product's internal temperature reaches approximately 90°C

A Statistical analysis was conducted in MATLAB using an ANOVA test to evaluate the impacts of temperature and baking time on color change. The results confirm that baking temperature have a significant effect on total color change ($p<0.05$). The findings indicate that higher baking temperatures lead to greater overall color variation. Moreover, baking temperature have a more significant influence than baking time on total color variation.

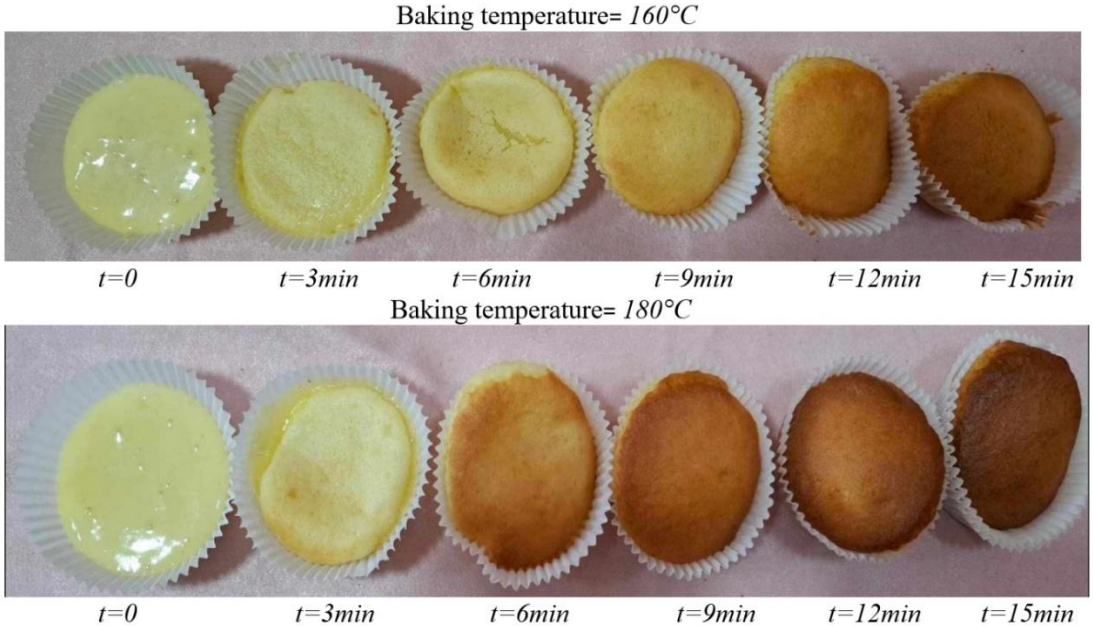

Figure 11. Color change of the cupcake surface during baking in an air fryer at 160°C and 180°C.

Seranthian and Datta (2023) found that in a conventional oven, no considerable browning occurs until approximately 16 minutes at 167.7°C and 190.6°C. However, in our study, optimal browning was achieved in 15 minutes at 160°C and 180°C (Figure 11), demonstrating that baking in an air fryer significantly reduces baking time while maintaining desirable color development. This illustrates how air fryers outperform traditional ovens in terms of heat transfer speed and baking ability. The efficiency may be due to the circulation of air under forced convection.

By incorporating a detailed heat and mass transfer approach, our numerical model successfully simulates real baking conditions, accurately predicting both when and how browning occurs. This ability to closely replicate experimental observations reinforces the crucial role of numerical simulations in analyzing the physical and chemical transformations that take place during baking.

9. CONCLUSION

This paper presents a mathematical model for understanding heat transport mechanisms, phase transitions, and quality changes occurring during cupcake baking in an air fryer. To provide a full assessment of heat and mass transmission, the model incorporates forced convection and radiation, in addition to conduction and natural convection considered in previous models.

The results demonstrate that forced convection and radiation significantly enhance heat transfer, reducing baking time. Temperature profiles showed distinct heating phases, with significant moisture loss followed by a stabilizing period as evaporation declined. Our model captured phase transitions and gas emissions, revealing that water evaporation occurs rapidly at the beginning, followed by water vapor and CO_2 formation, leading to volume expansion and texture development. To better assess the thermal impact of baking, we analyzed the cooking value (CV), a parameter derived by analogy to the sterilization value, which quantifies the cumulative thermal effect during the process. The CV analysis demonstrates that higher evaporation rates enhance heat transfer efficiency, resulting in faster cooking. Also, porosity evolution initially enhances heat transfer but later stabilizes, reducing efficiency.

To validate our model using MATLAB-based statistical analysis, experiments measurements of color change were conducted and compared to numerical simulations. The results showed excellent agreement with R^2 value of 0.996, confirming the model's accuracy. The ANOVA statistical analysis revealed that baking temperature has a more significant impact than baking time on total color variation $(p < 0.05)$. Higher temperatures accelerated browning

reactions due to enhanced Maillard reactions and caramelization, leading to faster and more pronounced color development.

Compared to previous studies utilizing conventional ovens, our findings highlight the efficiency of air fryers, offering optimized heat transfer, reduced baking time, and improved color formation. These insights contribute to the optimization of air frying parameters, providing a foundation for further studies on advanced baking technologies.

Table 3. Nomenclature.

Symbol	Description	Unit
ΔE	Total color variation	-
T	Temperature	°C
t	Time	Min
k	Kinetic coefficient	-
ρ	Density	Kg/m^3
C_p	Specific heat capacity	J/kg.K
k_p	Thermal conductivity	W/m.K
h	Heat transfer coefficient	W/m.K
ε	Emissivity	-
σ	Stefan-Boltzmann constant	$W/m^2.K$
D	Diffusion coefficient	m^2/s
L	Characteristic length	M
V	Volume	m^3
r	Radius	m
α	Volume fraction	-
μ	Dynamic viscosity	Pa.s
g	Gravitational acceleration	m/s^2
Nu	Nusselt number	-
Gr	Grashof number	-
Pr	Prandtl number	-
Ra	Rayleigh number	-
sh	Sherwood number	-
Tb	Baking temperature	°C
Tf	Final temperature	°C
R	Ideal gas constant	J/mol.K
Ea	Activation energy	*kJ/mol*
Ea_{color}	Color activation energy	*kJ/mol*
k_0	Pre exponential factor	s^{-1}
z	Thermal reference factor	-
CV	Cooking value	-
εp	Porosity	-
C_l	Liquid water fraction	-
C_v	Vapor water fraction	-
k_{evp}	Evaporation rate	s^{-1}

Funding: This study received no specific financial support.
Institutional Review Board Statement: Not applicable.
Transparency: The authors state that the manuscript is honest, truthful, and transparent, that no key aspects of the investigation have been omitted, and that any differences from the study as planned have been clarified. This study followed all writing ethics.
Competing Interests: The authors declare that they have no competing interests.
Authors' Contributions: All authors contributed equally to the conception and design of the study. All authors have read and agreed to the published version of the manuscript.

REFERENCES

Azmi, M. M. Z., Ahmedov, A., & Taip, F. S. (2020). Experimental studies and mathematical modeling on the effects of rapid airflow and baking temperature during baking. *Emirates Journal of Food and Agriculture, 32*(6), 469-478. https://doi.org/10.9755/ejfa.2020.v32.i6.2117

Bazinet, L., & Castaigne, F. (2019). *Food engineering concepts: Associated processes, applications to food preservation and processing (2nd updated and expanded ed.)*. Canada: *University of Montreal Press.*

Cevoli, C., Panarese, V., Catalogne, C., & Fabbri, A. (2020). Estimation of the effective moisture diffusivity in cake baking by the inversion of a finite element model. *Journal of Food Engineering, 270*, 109769. https://doi.org/10.1016/j.jfoodeng.2019.109769

El Helou, P., Le Bideau, P., Fuentes, A., & Glouannec, P. (2024). Experimental and numerical investigations of cake baking in mold. *Journal of Food Engineering, 382*, 112215. https://doi.org/10.1016/j.jfoodeng.2024.112215

El Helou, P. E., Bideau, P. L., Fuentes, A., & Glouannec, P. (2024). Numerical modelling of heat and mass transfer during cake baking. *Journal of Physics: Conference Series, 2766*, 012088. https://doi.org/10.1088/1742-6596/2766/1/012088

Feyissa, A. H., Gernaey, K., Ashokkumar, S., & Adler-Nissen, J. (2011). Modelling of coupled heat and mass transfer during a contact baking process. *Journal of Food Engineering, 106*(3), 228-235. https://doi.org/10.1016/j.jfoodeng.2011.05.014

Feyissa, A. H., Gernaey, K. V., & Adler-Nissen, J. (2012). Uncertainty and sensitivity analysis: Mathematical model of coupled heat and mass transfer for a contact baking process. *Journal of Food Engineering, 109*(2), 281-290. https://doi.org/10.1016/j.jfoodeng.2011.09.012

Khatir, Z., Paton, J., Thompson, H., Kapur, N., Toropov, V., Lawes, M., & Kirk, D. (2012). Computational fluid dynamics (CFD) investigation of air flow and temperature distribution in a small scale bread-baking oven. *Applied Energy, 89*(1), 89-96. https://doi.org/10.1016/j.apenergy.2011.02.002

Lee, Y., & Lee, K.-G. (2024). Effects of pan-and air fryer-roasting on volatile and umami compounds and antioxidant activity of dried laver (Porphyra dentata). *Food Chemistry, 458*, 140289. https://doi.org/10.1016/j.foodchem.2024.140289

Li, Y., Liu, H., Xie, L., & He, X. (2015). Mathematical modeling of heat distribution for the pan in a baking oven. *Advance Journal of Food Science and Technology, 8*(10), 747-750.

Mior Zakuan Azmi, M., Taip, F. S., Mustapa Kamal, S. M., & Chin, N. L. (2019). Effects of temperature and time on the physical characteristics of moist cakes baked in air fryer. *Journal of Food Science and Technology, 56*, 4616-4624. https://doi.org/10.1007/s13197-019-03926-z

Mołczan, T., & Cyklis, P. (2023). Impact of the evaporation temperature on the air drying rate for a finned heat exchanger. *Energies, 16*(5), 2132. https://doi.org/10.3390/en16052132

Mosalam, H. (2021). Digital modeling of heat transfer during the baking process. *Modelling and Simulation in Engineering, 2021*(1), 8957148. https://doi.org/10.1155/2021/8957148

Murzaini, N. M. N., Taip, F. S., Ab Aziz, N., & Abd Rahman, N. A. (2020). Effect of pre-treatment in producing pumpkin powder using air fryer and its application in 'Bingka'baking. *Current Research in Nutrition and Food Science Journal, 8*(1), 48-64.

Nicolas, V., Salagnac, P., Glouannec, P., Jury, V., Boillereaux, L., & Ploteau, J. P. (2010). *Modeling heat and mass transfer in bread during baking*. Paper presented at the Comsol Conference.

Sakin-Yilmazer, M., Kaymak-Ertekin, F., & Ilicali, C. (2012). Modeling of simultaneous heat and mass transfer during convective oven ring cake baking. *Journal of Food Engineering, 111*(2), 289-298. https://doi.org/10.1016/j.jfoodeng.2012.02.020

Sakin, M., Kaymak-Ertekin, F., & Ilicali, C. (2007). Modeling the moisture transfer during baking of white cake. *Journal of Food Engineering, 80*(3), 822-831. https://doi.org/10.1016/j.jfoodeng.2006.07.011

Seranthian, K., & Datta, A. (2023). Dynamics of cupcake baking: Coupled multiphase heat and mass transport in a deformable porous material. *Chemical Engineering Science, 277*, 118802. https://doi.org/10.1016/j.ces.2023.118802

Yang, W., Long, L., Zhang, L., Xu, K., Huang, Z., & Ye, H. (2025). Heat and mass transfer and deformation during chiffon cake baking. *Journal of Food Engineering, 388*, 112361. https://doi.org/10.1016/j.jfoodeng.2024.112361

Zanoni, B., Peri, C., & Bruno, D. (1995). Modelling of browning kinetics of bread crust during baking. *LWT-Food Science and Technology, 28*(6), 604-609. https://doi.org/10.1016/0023-6438(95)90008-X

Zhang, J., Datta, A., & Mukherjee, S. (2005). Transport processes and large deformation during baking of bread. *AIChE Journal, 51*(9), 2569-2580. https://doi.org/10.1002/aic.10518

APPENDIX

Table 1. Thermo-physical properties used in the mathematical model.

Density	$\rho_{prot} = 1.3300 * 10^3 - 0.5184.T$ $\rho_{carb} = 1.5991 * 10^2 - 0.31046.T$ $\rho_{fat} = 9.2559 * 10^2 - 0.41757.T$ $\rho_{\text{dry}} = (\rho_{\text{carb}}.w_{\text{carb}} + \rho_{\text{prot}}.w_{\text{prot}} + \rho_{\text{fat}}.w_{\text{fat}} + \rho_{\text{fiber}}.w_{\text{fiber}})/w_{dry}$ $\rho_w^l = 9{,}9718 * 10^2 + 3{,}1439 * 10^{-3}T - 3{,}7574.10^{-3}T^2$ $\rho_w^v = \frac{P.M_{H_2O}}{RT}$ $\rho_{fluid} = C_l.\rho_l + C_v.\rho_v + C_{CO_2}.\rho_{CO_2}$ $C_{CO_2} + C_l + C_v = 1$ $\rho_{fluid} = C_l.\rho_l + C_v.\rho_v + (1 - C_l - C_v).\rho_{CO_2}$ $\rho_{prod} = (1 - \varepsilon).\rho_{dry} + \varepsilon.\rho_{fluid}$
Specific heat	$C_{p,prot} = 2.0082 + 1.2089 * 10^{-3} - 1.3129 * 10^{-6}T^2 C_{p,carb}$ $= 1.5488 + 1.9625 * 10^{-3}T - 5.9399 * 10^{-6}T^2$ $C_{p,fat} = 1.9842 + 1.4733 * 10^{-3}T - 4.8008 * 10^{-6}T^2$ $C_{p,fiber} = 1{,}8459 + 1{,}8306 * 10^{-3} - 4{,}6509 * 10^{-6}T^2 Cp_{\text{dry}}$ $= (Cp_{\text{carb}}.w_{\text{carb}} + Cp_{\text{prot}}.w_{\text{prot}} + Cp_{\text{fat}}.w_{\text{fat}} + Cp_{\text{fiber}}.w_{\text{fiber}})/w_{dry}$ $C_{p,l} = 4.1762 + 9.0862 * 10^{-5}T + 5.4731 * 10^{-6}T^2$ $\frac{C_{p,v}}{R} = 3.49708 + 1.5226033 * 10^{-3}T + 2.2301684 * 10^{-8}T^2 - 5.9706577 * 10^{-11}T^3$ $\frac{Cp_{CO2}}{R} = 3.28677 + 5.1201479 * 10^{-3}T + 2.2351997 * 10^{-6}T^2 - 3.3521927 * 10^{-10}T^3$ $Cp_{fluid} = C_l.Cp_l + C_v.Cp_v + C_{CO_2}.Cp_{CO_2}$ $Cp_{fluid} = C_l.Cp_l + C_v.Cp_v + (1 - C_l - C_v).Cp_{CO_2}$ $Cp_{prod} = (1 - \varepsilon).Cp_{dry} + \varepsilon.Cp_{fluid}$